A Mitochondrial Pyruvate Carrier Required for Pyruvate Uptake in Yeast, *Drosophila*, and Humans

Daniel K. Bricker[1,*], **Eric B. Taylor**[2,*], **John C. Schell**[2,*], **Thomas Orsak**[2,*], **Audrey Boutron**[3], **Yu-Chan Chen**[2], **James E. Cox**[4], **Caleb M. Cardon**[2], **Jonathan G. Van Vranken**[2], **Noah Dephoure**[5], **Claire Redin**[6], **Sihem Boudina**[7], **Steven P. Gygi**[5], **Michèle Brivet**[3], **Carl S. Thummel**[1], and **Jared Rutter**[2,†]

[1]Department of Human Genetics, University of Utah School of Medicine, Salt Lake City, UT 84112, USA

[2]Department of Biochemistry, University of Utah School of Medicine, Salt Lake City, UT 84112, USA

[3]Laboratoire de Biochimie, AP-HP Hôpital de Bicêtre, Le Kremlin Bicêtre, France

[4]Metabolomics Core Research Facility, University of Utah School of Medicine, Salt Lake City, UT 84112, USA

[5]Department of Cell Biology, Harvard Medical School, Boston, MA 02115, USA

[6]Institut de Genetique et de Biologie Moleculaire et Cellulaire (IGBMC), Strasbourg, France

[7]Department of Medicine, University of Utah School of Medicine, Salt Lake City, UT 84112, USA

Abstract

Pyruvate constitutes a critical branch point in cellular carbon metabolism. We have identified two proteins, Mpc1 and Mpc2, as essential for mitochondrial pyruvate transport in yeast, *Drosophila*, and humans. Mpc1 and Mpc2 associate to form an ~150-kilodalton complex in the inner mitochondrial membrane. Yeast and *Drosophila* mutants lacking *MPC1* display impaired pyruvate metabolism, with an accumulation of upstream metabolites and a depletion of tricarboxylic acid cycle intermediates. Loss of yeast Mpc1 results in defective mitochondrial pyruvate uptake, and silencing of *MPC1* or *MPC2* in mammalian cells impairs pyruvate oxidation. A point mutation in *MPC1* provides resistance to a known inhibitor of the mitochondrial pyruvate carrier. Human genetic studies of three families with children suffering from lactic acidosis and hyperpyruvatemia revealed a causal locus that mapped to *MPC1*, changing single amino acids that are conserved throughout eukaryotes. These data demonstrate that Mpc1 and Mpc2 form an essential part of the mitochondrial pyruvate carrier.

Pyruvate occupies a pivotal node in the regulation of carbon metabolism as it is the end product of glycolysis and a major substrate for the tricarboxylic acid (TCA) cycle in mitochondria. Pyruvate lies at the intersection of these catabolic pathways with anabolic pathways for lipid synthesis, amino acid biosynthesis, and gluconeogenesis. As a result, the failure to correctly partition carbon between these fates lies at the heart of the altered metabolism evident in diabetes, obesity, and cancer (1, 2). Owing to the fundamental

importance of pyruvate, the mitochondrial pyruvate carrier (MPC) has been studied extensively (3, 4). This included the discovery that α-cyanocinnamate analogs, such as UK-5099, act as specific and potent inhibitors of carrier activity (5). In spite of this characterization, however, the gene or genes that encode the mitochondrial pyruvate carrier remain unknown (6, 7).

As part of an ongoing effort to characterize mitochondrial proteins that are conserved through evolution, we initiated studies of the MPC protein family (originally designated BRP44 and BRP44L in humans) (8). This family contains three members in *Saccharomyces cerevisiae*, encoded by *YGL080W*, *YHR162W*, and *YGR243W*, hereafter referred to as *MPC1*, *MPC2*, and *MPC3*, respectively. Mpc2 and Mpc3 are 79% identical in amino acid sequence and appear to be the product of a recent gene duplication event. Mpc1, Mpc2, and Mpc3 colocalize with mitochondria (Fig. 1A and fig. S2A), consistent with published mitochondrial proteomic studies (9, 10). The mitochondrial localization of Mpc1 and Mpc2 was confirmed by biochemical fractionation (Fig. 1B). Mpc1, Mpc2, and Mpc3 were enriched in mitochondrial membranes (fig. S2B), consistent with the presence of predicted transmembrane domains in their sequences (fig. S1). Mpc1 and Mpc2 were resistant to protease treatment unless the mitochondrial outer membrane was ruptured (Fig. 1B and fig. S2C), implying that they are embedded in the mitochondrial inner membrane. Chromatographic purification of tagged variants of Mpc1 and Mpc2, followed by mass spectrometry, revealed that Mpc2 and Mpc3 were among the major interacting proteins of Mpc1, and Mpc1 and Mpc3 were among the major interacting proteins of Mpc2 (table S1). Consistent with this, immunoprecipitation of tagged Mpc1 copurified Mpc2 and vice versa (Fig. 1C, lanes 3 and 4). In addition, Mpc2 can interact with itself (Fig. 1C, lane 8), whereas an Mpc1 homotypic interaction was not detected (Fig. 1C, lane 7). Blue native–polyacrylamide gel electrophoresis showed that both Mpc1 and Mpc2 migrated as part of an ~150-kD complex (fig. S2D). Loss of Mpc2 prevented Mpc1 from migrating in this complex, whereas an *mpc1Δ* strain showed elevated Mpc2 complex formation (fig. S2E). We conclude that Mpc1 and Mpc2 form a multimeric complex embedded in the mitochondrial inner membrane, with Mpc2 likely being the major structural subunit.

Mutant yeast strains were subjected to a variety of growth conditions. The *mpc1Δ* and *mpc2Δ* cells displayed mild growth defects on non-fermentable carbon sources like glycerol, with greater effects on glucose medium (fig. S3) and a strong growth defect in the absence of leucine (Fig. 1D). In contrast, *mpc3Δ* mutant displayed no apparent growth phenotypes. Yeast, *Drosophila*, or human *MPC1* orthologs, but not human *MPC2*, could rescue the *mpc1Δ* growth phenotype (Fig. 1E), indicating that Mpc1 function is conserved through evolution.

To analyze the physiological function of MPCs in a multicellular animal, we extended our studies to the *Drosophila* ortholog of MPC1 (dMPC1; encoded by *CG14290*), which also localized to mitochondria (fig. S4). Analogous to yeast *mpc1Δ* mutants, *dMPC1* mutants (fig. S5) were viable on standard food, but sensitive to a carbohydrate-only diet, with rapid lethality after transfer to a sucrose medium (Fig. 2A). Whereas the amount of adenosine 5′-triphosphate (ATP) was reduced in *dMPC1* mutants (Fig. 2C), along with triacylglycerol (TAG) and protein (fig. S6, B and C), the amounts of carbohydrates were elevated, including the circulating sugar trehalose (Fig. 2D), glucose (Fig. 2E), fructose, and glycogen (fig. S6, A and D). These results suggest that *dMPC1* mutants are defective in carbohydrate metabolism and may consume stored fat and protein for energy. Consistent with this, the lethality of *dMPC1* mutants on the sugar diet was rescued by expression of the wild-type gene in tissues that depend heavily on glucose metabolism: the fat body, muscle, and neurons (Fig. 2B).

Metabolomic analyses revealed that the concentration of pyruvate was highly elevated, whereas TCA cycle intermediates were significantly depleted in *dMPC1* mutants on the sugar diet (Fig. 2F). Similarly, the amounts of glycine and serine, which can interconvert with glycolytic intermediates, were elevated in the mutants on the sugar diet (fig. S6E), whereas glutamate, aspartate, and proline, which can interconvert with TCA cycle intermediates, were depleted under these conditions (fig. S6F). Consistent with this, metabolomic analysis of *mpc1Δ* and *mpc2Δ* yeast mutants revealed elevated pyruvate concentrations (Fig. 3A), depletion of malate (fig. S7), depleted acetyl–coenzyme A (CoA), and elevated CoA concentrations (Fig. 3B). Taken together, these results suggest that *MPC1* mutants are unable to efficiently convert cytosolic pyruvate to mitochondrial acetyl-CoA to drive the TCA cycle and ATP production.

These phenotypes could arise from either a defect in mitochondrial pyruvate uptake or the conversion of mitochondrial pyruvate into acetyl-CoA by the pyruvate dehydrogenase (PDH) complex. Yeast lacking Mpc1, however, had nearly wild-type PDH activity, unlike the strong decrease seen in *pda1Δ* mutants (Fig. 3C), which lack PDH function (11). A decrease in PDH activity also does not explain the growth defect of *mpc1Δ* mutants, which is more severe than that of the *pda1Δ* mutant (fig. S8). However, combining the *mpc1Δ* allele with a deletion for *mae1*, which encodes a malic enzyme that converts malate to pyruvate in the mitochondrial matrix (12), revealed a profound growth defect on glucose medium that was completely rescued by plasmid expression of either *MAE1* or *MPC1* (Fig. 3D). Notably, mitochondria from the *mpc1Δ* mutant displayed almost no uptake of ^{14}C-pyruvate, which could be fully rescued by plasmid expression of wild-type *MPC1* (Fig. 3E). Moreover, Mpc1 appears to be a key target for UK-5099, which is an inhibitor of the mitochondrial pyruvate carrier (5). The *mae1Δ mpc1Δ* double mutant displayed reduced growth on glucose medium lacking leucine, and this phenotype could be effectively rescued by transgenic expression of wild-type *MPC1* in the absence, but not the presence, of UK-5099 (Fig. 3F). By screening for *MPC1* mutants that could grow in the presence of UK-5099, we recovered an Asp^{118}→Gly (D118G) substitution in Mpc1 that conferred UK-5099 resistance (Fig. 3F). Moreover, whereas ^{14}C-pyruvate uptake into mitochondria expressing wild-type *MPC1* was almost completely inhibited by UK-5099, efficient pyruvate uptake that is resistant to UK-5099 was recovered upon expression of *MPC1-D118G* (Fig. 3G). We conclude that Mpc1 is a key component of the mitochondrial pyruvate carrier that corresponds to the activity studied for decades by Halestrap and others (5, 13).

Depletion of *MPC1* in mouse embryonic fibroblasts (fig. S9A) caused a modest decrease in pyruvate-driven oxygen consumption under basal conditions, and a stronger reduction in the presence of carbonyl cyanide-*p*-trifluoromethoxyphenylhydrazone (FCCP), which stimulates maximal respiration (Fig. 4A). Similar results were also seen upon silencing *MPC2* (Fig. 4B and fig. S9A). This suppression of pyruvate oxidation, which occurred without affecting components of the oxidative phosphorylation machinery (fig. S9, B and C), suggests that mammalian Mpc1 and Mpc2 mediate mitochondrial pyruvate uptake in a manner similar to that seen in yeast and *Drosophila*.

We have previously described a French-Algerian family with two offspring that exhibited a devastating defect in mitochondrial pyruvate oxidation (14) (Fig. 4C, family 1). We subsequently discovered two additional families, each with one affected child who displayed a similar, but less severe, phenotype (Fig. 4C, families 2 and 3). Linkage analysis and homozygosity mapping allowed us to focus on one candidate region on chromosome 6 (163,607,637 to 166,842,083, GRCh37/hg19). This interval contained 10 potential candidate genes: *PACRG*, *QKI*, *C6orf118*, *PDE10A*, *SDIM1*, *T*, *PRR18*, *SFT2D1*, *RPS6KA2*, and *BRP44L*, which is the human *MPC1*. DNA sequencing of the exons and intron/exon boundaries of the *MPC1* gene in fibroblasts from the affected patients in families 2 and 3

revealed the same molecular lesion, c.236T→A, causing a predicted p.Leu^{79}→His (L79H) alteration (Fig. 4D). Analysis of DNA from family 1 revealed a distinct sequence change, c. 289C→T, which resulted in a predicted p.Arg^{97}→Trp (R97W) mutation (Fig. 4D). Both of the affected residues are conserved through evolution between *MPC1* orthologs, and Arg^{97} is conserved among both *MPC1* and *MPC2* orthologs (fig. S1).

Cells from the affected individuals in families 1 and 2 exhibited impaired basal and FCCP-stimulated pyruvate oxidation (Fig. 4E), whereas glutamine-driven oxygen consumption was normal or elevated, demonstrating that they have not acquired a generalized impairment of mitochondrial respiration (Fig. 4E). As expected, expression of wild-type human *MPC1* in the cells from family 2 (Fig. 4F) or family 1 (Fig. 4G) either completely or partially rescued the defect in FCCP-induced pyruvate oxidation. Moreover, expression of the *MPC1-Leu79His* allele was less effective at suppressing the yeast *mpc1Δ* growth defect relative to wild-type human *MPC1* (Fig. 4H), and the stronger *MPC1-Arg97Trp* allele was essentially inactive (Fig. 4H), suggesting that *MPC1* function is evolutionarily conserved from yeast to humans.

The data presented here demonstrate that the Mpc1-Mpc2 complex is an essential component of the mitochondrial pyruvate carrier in yeast, flies, and mammals. This is consistent with experiments performed in rat liver, heart, and castor beans, which implicated proteins of 12 to 15 kD in mitochondrial pyruvate uptake (15)—similar to the molecular masses of Mpc1 (15 kD), Mpc2 (14 kD), and Mpc3 (16 kD). Although these individual sizes are relatively small, Mpc1 and Mpc2 form a complex of ~150 kD, suggesting that an oligomeric structure mediates pyruvate transport. The demonstration that Mpc1 and Mpc2 are sufficient to promote pyruvate uptake in a heterologous system provides further evidence that they constitute an essential pyruvate transporter (16). Finally, the degree to which carbohydrates are imported into mitochondria and converted into acetyl-CoA is a critical step in normal glucose oxidation as well as the onset of diabetes, obesity, and cancer. Thus, like PDH, which is controlled by allostery and posttranslational modification (17), the mitochondrial import of pyruvate is likely to be precisely regulated (18, 19). The identification of Mpc1 and Mpc2 as critical for mitochondrial pyruvate transport provides a new framework for understanding this level of metabolic control, as well as new directions for potential therapeutic intervention.

Supplementary Material

Refer to Web version on PubMed Central for supplementary material.

Acknowledgments

References and Notes

1. Hanahan D, Weinberg RA. Cell. 2011; 144:646. [PubMed: 21376230]

2. Kahn SE, Hull RL, Utzschneider KM. Nature. 2006; 444:840. [PubMed: 17167471]

3. Halestrap AP, Denton RM. Biochem J. 1974; 138:313. [PubMed: 4822737]

4. Halestrap AP. Biochem J. 1978; 172:377. [PubMed: 28726]

5. Halestrap AP. Biochem J. 1975; 148:85. [PubMed: 1156402]

6. Todisco S, Agrimi G, Castegna A, Palmieri F. J Biol Chem. 2006; 281:1524. [PubMed: 16291748]

7. Hildyard JC, Halestrap AP. Biochem J. 2003; 374:607. [PubMed: 12887330]

8. Jiang M, et al. Mol Biol Rep. 2009; 36:215. [PubMed: 18026869]

9. Pagliarini DJ, et al. Cell. 2008; 134:112. [PubMed: 18614015]

10. Sickmann A, et al. Proc Natl Acad Sci USA. 2003; 100:13207. [PubMed: 14576278]

11. Steensma HY, Holterman L, Dekker I, van Sluis CA, Wenzel TJ. Eur J Biochem. 1990; 191:769. [PubMed: 2202601]

12. Boles E, de Jong-Gubbels P, Pronk JT. J Bacteriol. 1998; 180:2875. [PubMed: 9603875]

13. Papa S, Paradies G. Eur J Biochem. 1974; 49:265. [PubMed: 4459142]

14. Brivet M, et al. Mol Genet Metab. 2003; 78:186. [PubMed: 12649063]

15. Thomas AP, Halestrap AP. Biochem J. 1981; 196:471. [PubMed: 7316989]

16. Herzig S, et al. Science. 2012; 337:93. [PubMed: 22628554]

17. Harris RA, Bowker-Kinley MM, Huang B, Wu P. Adv Enzyme Regul. 2002; 42:249. [PubMed: 12123719]

18. Zwiebel FM, Schwabe U, Olson MS, Scholz R. Biochemistry. 1982; 21:346. [PubMed: 7074018]

19. Rognstad R. Int J Biochem. 1983; 15:1417. [PubMed: 6653863]

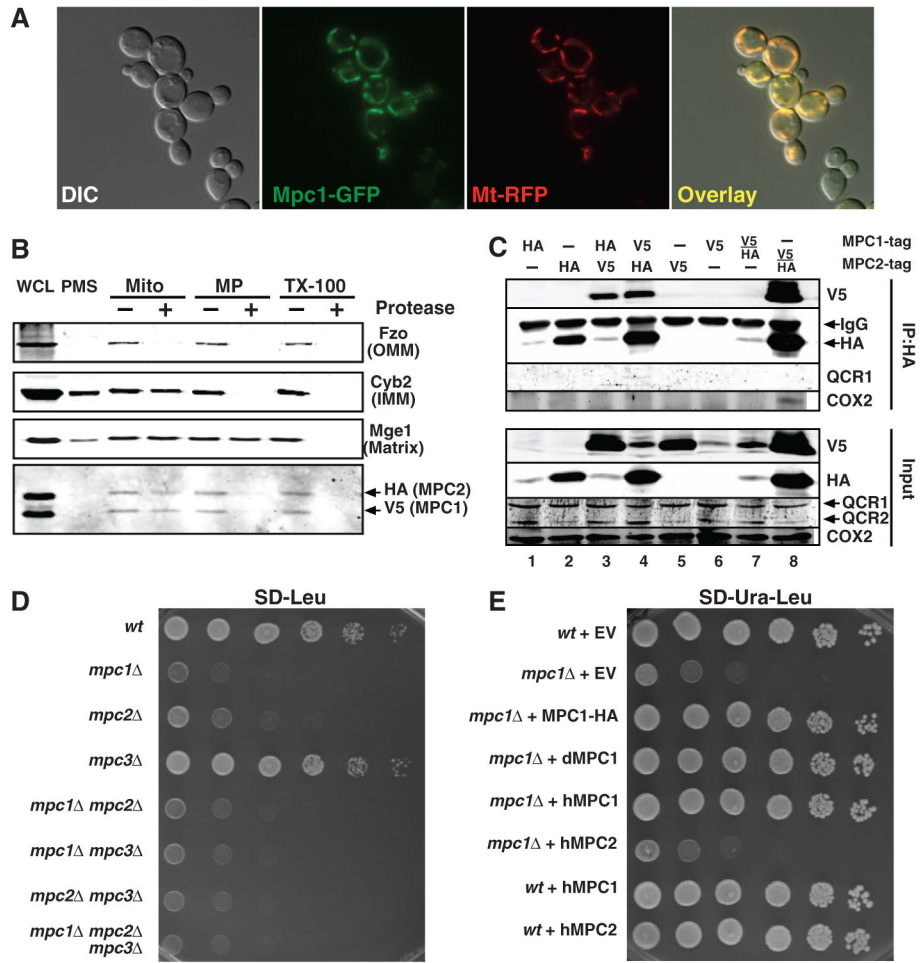20. Materials and methods are available as supplementary materials on *Science* Online.

Fig. 1.
Mpc1 and Mpc2 are evolutionarily conserved mitochondrial inner-membrane proteins. (**A**) Mpc1 labeled with green fluorescent protein (Mpc1-GFP) and mitochondrial targeted red fluorescent protein (MtRFP) coexpressed in yeast cells. DIC, differential interference contrast. (**B**) Intact mitochondria, hypotonic-swollen mitoplasts, and TritonX-100–solubilized mitochondria from a strain expressing Mpc1-V5 and Mpc2-His$_6$/HA$_2$ with (+) or without (−) proteinase K incubation. An immunoblot of extracts using the indicated antibodies with the whole-cell lysate (WCL) and postmitochondrial supernatant (PMS) is shown. Mge1, Cyb2, and Fzo1 are matrix, intermembrane space, and outer-membrane proteins, respectively. (**C**) Immunoprecipitations from mitochondrial extracts from *mpc1Δ mpc2Δ* cells expressing Mpc1 and Mpc2 tagged as indicated. Immunoblot of either immunoprecipitate (IP:HA) or input is shown (HA, hemagglutinin). QCR1 and 2 (ubiquinol–cytochrome c reductase complex core protein 1 and 2) along with Cox II (cytochrome c oxidase subunit 2) are controls for the specificity of the immunoprecipitation. (**D**) Serial dilutions of the indicated yeast strains spotted on synthetic media lacking leucine and grown at 30°C for 24 hours. (**E**) Serial dilutions of indicated strains spotted on synthetic media lacking leucine and grown at 30°C for 48 hours. *wt*, wild type; EV, empty vector.
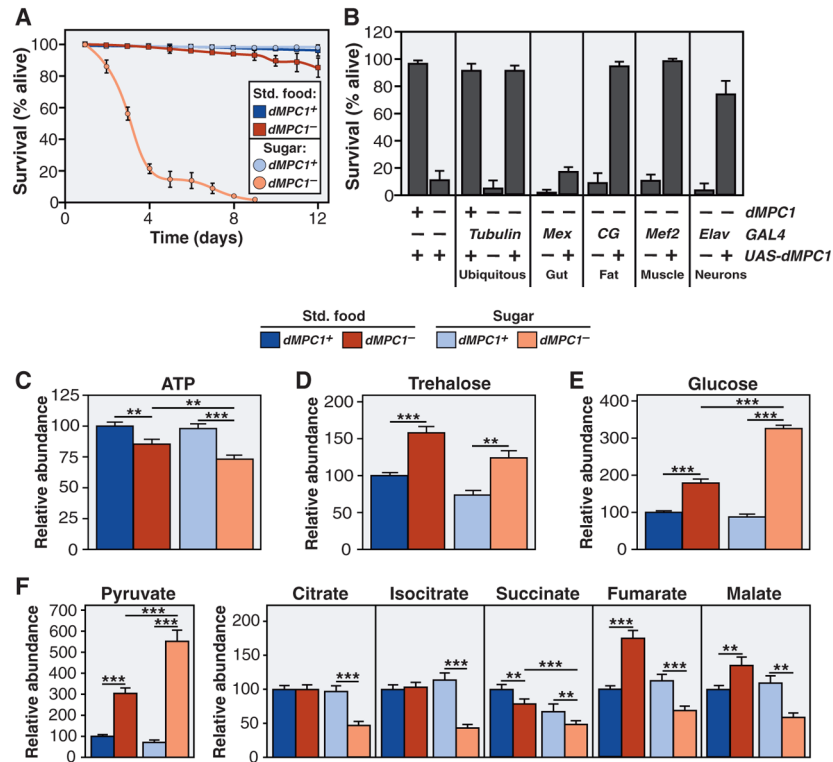
Fig. 2.
dMPC1 is required for pyruvate metabolism in *Drosophila.* (**A**) Percentage of living control
(*dMPC1⁺*) or *dMPC1* mutant (*dMPC⁻*) flies after transfer to standard laboratory medium
(std. food) or to media containing only sugar. (**B**) Percentage of living *dMPC1⁺* or *dMPC⁻*
flies carrying the indicated GAL4 and UAS transgenes on sugar media after 8 days. (**C** to **E**)
Relative concentration of ATP (C), trehalose (D), and glucose (E) in extracts from *dMPC1⁺*
or *dMPC⁻* flies on the indicated diet after either 2 days (D and E) or 3 days (C). (**F**) Relative
abundance of pyruvate and TCA cycle intermediates in *dMPC1⁺* or *dMPC⁻* flies after 2 days
on the indicated diet as measured by gas chromatography–mass spectrometry. *$P < 0.05$,
**$P < 0.01$, and ***$P < 0.001$ (Student's *t* test). Data are shown as mean ± SEM.
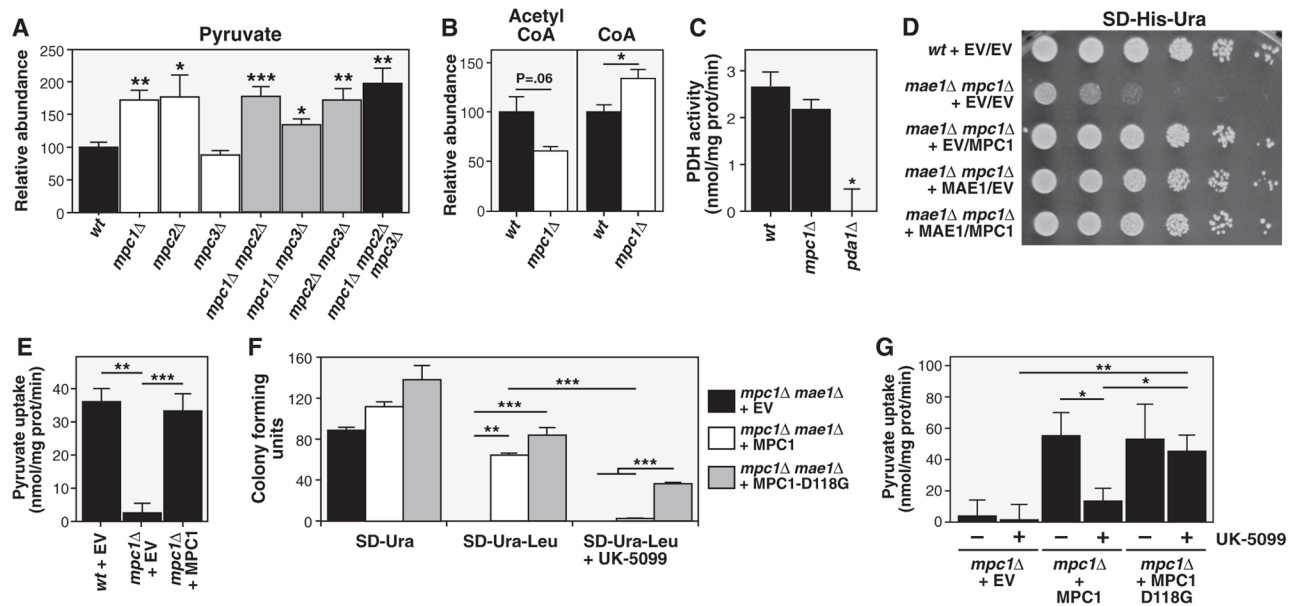
Fig. 3.
MPC1 is required for mitochondrial pyruvate uptake. (**A**) Relative abundance of pyruvate in the indicated strains. *P* values relative to *wt*. (**B**) Relative abundance of acetyl-CoA and CoA in the indicated strains. (**C**) Mitochondrial pyruvate dehydrogenase activity in the indicated strains. *P* value relative to *wt* and *mpc1Δ*. (**D**) Serial dilutions of the indicated strain on glucose medium grown at 30°C for 48 hours. (**E**) Uptake of ^{14}C-pyruvate into mitochondria purified from either *wt* or *mpc1Δ* cells containing the indicated plasmid. *P* value relative to *wt + EV* and *mpc1Δ + MPC1*. (**F**) *Mae1Δ mpc1Δ* cells transformed with the indicated plasmid and plated on media containing or lacking combinations of leucine or UK-5099. (**G**) Uptake of ^{14}C-pyruvate into mitochondria isolated from the *mpc1Δ* strain containing the indicated plasmid in the presence or absence of UK-5099. ***$P < 0.001$, **$P < 0.01$, *$P < 0.05$; NS, not significant (Student's *t* test). Data are shown as mean ± SEM.
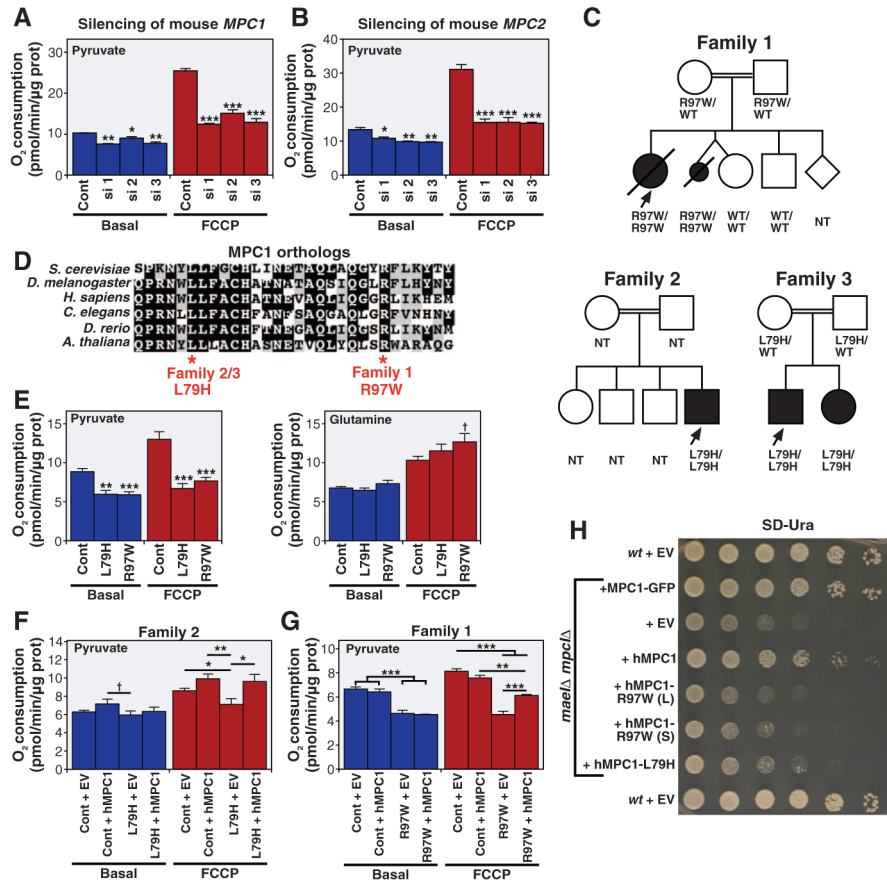
Fig. 4.
Mammalian *MPC1* and *MPC2* are required for normal pyruvate metabolism. (**A** and **B**) Pyruvate-driven respiration in mouse embryonic fibroblasts under basal and FCCP-stimulated conditions in cells transfected with either control (Cont) small interfering RNAs (siRNAs) or three different siRNAs (si 1–3) targeted to either *MPC1* (A) or *MPC2* (B). *P* values relative to control. (**C**) Pedigrees of families 1, 2, and 3. Circles indicate females; squares, males; and diamonds, unknown sex. Black indicates deceased and white, living. Arrows mark individuals from whom fibroblasts were obtained. (**D**) The protein region of MPC1 containing the predicted amino acid substitutions from all three families aligned by ClustalW. Single-letter abbreviations for the amino acid residues are as follows: A, Ala; C, Cys; D, Asp; E, Glu; F, Phe; G, Gly; H, His; I, Ile; K, Lys; L, Leu; M, Met; N, Asn; P, Pro; Q, Gln; R, Arg; S, Ser; T, Thr; V, Val; W, Trp; and Y, Tyr. *Saccharomyces cerevisiae, Drosophila melanogaster, Homo sapiens, Caenorhabditis elegans, Danio rerio, Arabidopsis thaliana*. (**E**) Pyruvate- (left) and glutamine- (right) supported respiration of fibroblasts harboring either L79H or R97W *MPC1* mutations. (**F**) Pyruvate-supported respiration of either a control or an L79H patient cell line after transduction with the indicated vector. (**G**) Pyruvate-supported respiration of either a control or an R97W patient cell line after transduction with the indicated vector. (**H**) Serial dilutions of *wt* or *mae1Δ mpc1Δ* yeast strains carrying the indicated plasmid grown on medium lacking uracil for plasmid selection at 30°C for 40 hours. Both long (L) and short (S) forms of R97W were used (with or without exon 4). ***P < 0.001, **P < 0.01, *P < 0.05, †*P* < 0.10; NS, not significant (Student's *t* test). Data are shown as mean ± SEM.